

BioPro: On Difference-Aware Gender Fairness for Vision-Language Models

Yujie Lin^{1*}, Jiayao Ma^{1*}, Qingguo Hu¹, Derek F. Wong², Jinsong Su^{1†}

¹School of Informatics, Xiamen University

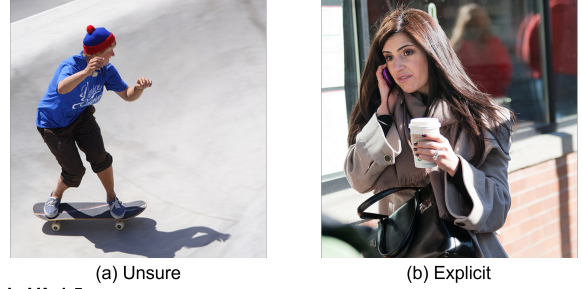
²Department of Computer and Information Science, University of Macau
linyujie@stu.xmu.edu.cn

Abstract

Vision-Language Models (VLMs) inherit significant social biases from their training data, notably in gender representation. Current fairness interventions often adopt a “difference-unaware” perspective that enforces uniform treatment across demographic groups. These approaches, however, fail to distinguish between contexts where neutrality is required and those where group-specific attributes are legitimate and must be preserved. Building upon recent advances in difference-aware fairness for text-only models, we extend this concept to the multimodal domain and formalize the problem of difference-aware gender fairness for image captioning and text-to-image generation. We advocate for selective debiasing, which aims to mitigate unwanted bias in neutral contexts while preserving valid distinctions in explicit ones. To achieve this, we propose BioPro (Bias Orthogonal Projection), an entirely **training-free** framework. BioPro identifies a low-dimensional gender-variation subspace through counterfactual embeddings and applies projection to selectively neutralize gender-related information. Experiments show that BioPro effectively reduces gender bias in neutral cases while maintaining gender faithfulness in explicit ones, thus providing a promising direction toward achieving selective fairness in VLMs. Beyond gender bias, we further demonstrate that BioPro can effectively generalize to continuous bias variables, such as scene brightness, highlighting its broader applicability.

1. Introduction

Large Language Models (LLMs) [1, 7] have demonstrated remarkable capabilities across diverse natural language tasks. However, their impressive fluency often comes with a significant drawback: social bias [31]. These models inherit and amplify patterns of bias from their large-scale training data, leading to unfair or stereotypical outputs [10, 24,



LLaVA-1.5

(a) The image features a young **man** wearing a blue shirt and a red hat, riding a skateboard on a ramp ...

(b) The image features a **woman** wearing a coat and scarf, talking on her cell phone. She is holding a cup, possibly a coffee ...

BioPro (ours)

(a) The image features a **person** wearing a blue shirt and a red hat, riding a skateboard on a ramp ... (*debaised*)

(b) The image features a **woman** wearing a coat and scarf, talking on her cell phone. She is holding a cup, possibly a coffee ... (*unchanged*)

Figure 1. BioPro can selectively perform debiasing primarily on neutral samples labeled as unsure gender.

[36, 40]. Existing fairness research on LLMs has largely adopted a *difference-unaware* perspective, where fairness is operationalized as treating all demographic groups identically regardless of context. While such approaches can reduce overt disparities, they often neglect the nuanced circumstances where group differences are legitimate or even necessary to recognize [42].

Difference-aware fairness offers an alternative perspective that explicitly acknowledges the importance of contextual differentiation. As argued in [42], fair behavior does not always entail uniform treatment across groups: in many real-world situations, fair outcomes require sensitivity to social, cultural, or legal distinctions. To this end, they introduce the notion of *difference awareness*, emphasizing that models should discern when it is contextually appropriate to treat groups differently (e.g., gender-specific legal exemptions) and when uniformity is required. Through a comprehensive benchmark suite, they demonstrate that current LLMs though highly capable and well-aligned, often exhibit difference unawareness, failing to recognize meaningful group distinctions when they matter most.

*Equal contribution.

†Corresponding author.



Figure 2. An example of text-to-image generation. The figure shows eight images generated from the same prompt with fixed seeds ranging from 0 to 7. BioPro can help balance the gender distribution of the generated images.

While prior studies have focused on text-only settings, the same challenge persists and arguably intensifies in vision-language models (VLMs) [27, 37, 46]. VLMs jointly process multimodal information to perform tasks such as image captioning and text-to-image generation. In multimodal scenarios, fairness entails not only generating unbiased language or images but doing so in a way that is sensitive to visual or textual context. As shown in Fig. 1, when describing a person in a photo, a captioning model should avoid inferring gender for gender-ambiguous subjects, yet should faithfully preserve gender information when it is visually evident. Similarly, the problem can be extended to text-to-image generation. A neutral prompt (e.g., “a photo of a person who works as a doctor”) should yield a balanced gender distribution (Fig. 2), whereas an explicit prompt (e.g., “a photo of a female doctor”) should respect the specified gender identity. Motivated by these problems, we propose the notion of difference-aware gender fairness for VLMs, extending the concept of difference awareness from the text domain to multimodal learning. Our goal is to achieve selective debiasing, mitigating unwanted gender bias in neutral contexts while preserving intended gender semantics in explicit contexts. To this end, we formalize the problem of difference-aware fairness on two representative VLM tasks: image captioning and text-to-image generation. For each task, we define a set of constraints that balance three desirable properties: (i) neutral fairness (bias suppression for neutral inputs), (ii) explicit gender faithfulness (gender consistency for gender-explicit cases), and (iii) semantic preservation (maintaining task-relevant content).

Building on this formulation, we introduce a novel debiasing framework termed **Bias Orthogonal Projection (BioPro)**, which enables targeted removal of bias-related components from multimodal representations. The key idea is to identify a low-dimensional gender-variation subspace through paired counterfactual embeddings, and then perform orthogonal projection to selectively neutralize gender-related information. To avoid over-correction, we further introduce a projection-based selection mechanism that adapts debiasing strength according to the degree of gender expression in each sample. For text-to-image generation, where the output inherently contains gender attributes, we propose an additional calibration term to balance gender proportions in neutral prompts without erasing intended semantics in explicit ones. In particular, without the difference-aware setting, our method can generalize to other types of bias. BioPro is capable of handling non-discrete, continuous bias variables. For instance, when generating images of forests, the model tends to produce scenes with sufficient illumination while lacking samples under dim lighting conditions. In this case, environmental brightness serves as a continuous bias variable, which we refer to as scene bias. BioPro can effectively control the model to generate more scenes with lower brightness, and the illumination level can be flexibly adjusted through a hyperparameter. In summary, our contributions are three-fold:

- We firstly extend the concept of difference-aware fairness from LLMs to VLMs, providing a principled formulation for selective bias mitigation in multimodal tasks.
- We propose BioPro, an entirely **training-free** framework for both image captioning and generation, ensuring fairness without compromising semantic fidelity. To the best

of our knowledge, BioPro is the first method that introduces and effectively handles continuous bias variables in text-to-image generation tasks.

- Through comprehensive experiments, we demonstrate that BioPro effectively reduces gender bias in neutral cases while maintaining gender faithfulness in explicit ones, highlighting the feasibility of selective fairness in vision–language systems.

2. Related Works

Social Bias in VLMs. VLMs inevitably inherit social stereotypes from large-scale vision–language corpora, leading to reliance on contextual shortcuts (e.g., kitchen \rightarrow woman) [14, 45] and amplification of such biases during generation [16]. Although fine-tuning based debiasing strategies [11, 20, 21, 23, 41, 43] exist, they are often costly and model-specific, motivating growing interest in post-hoc (inference-time) interventions for their flexibility and generality. Such methods generally fall into three categories: (i) prompt-space interventions [3, 8, 20, 38]; (ii) representation-space interventions (e.g., via projection) [6, 9, 13, 19, 39]; and (iii) post-generation corrections, which adjust generated outputs after inference [17, 32].

Difference-aware Bias in LLMs. Recent work in LLMs by Wang et al. [42] challenges the notion of “fairness as blindness.” They formalize difference-aware fairness, arguing that models must distinguish between spurious stereotypes (e.g., nurse \rightarrow female) and legitimate, context-regulated differences (e.g., gender-specific medical descriptions). Moreover, Wang et al. [42] show that common debiasing techniques, such as moral self-correction prompts [12, 26, 35], tend to reduce difference awareness. Their results underscore a fundamental limitation of current bias mitigation paradigms: striving for demographic parity can erase legitimate contextual distinctions and paradoxically produce less fair outcomes in sensitive applications.

3. Difference-Aware Fairness for VLMs

In this section, we define the difference-aware gender fairness problem on two representative vision–language tasks: image captioning and text-to-image generation. The subscripts c and g denote captioning and generation, respectively.

3.1. Image Captioning

Consider an input image $x \in \mathcal{X}$ and a text prompt t_c . Given a VLM M_c , we obtain the caption of x as $y_c = M_c(x, t_c)$. For the input image set \mathcal{X} , we divide it into two subsets: the explicit set \mathcal{X}_e , which contains images with clearly identifiable gendered subjects, and the neutral set $\mathcal{X}_n = \mathcal{X} \setminus \mathcal{X}_e$, which includes images whose subjects’ gender is ambiguous or difficult to determine. For each image x , we extract

a multimodal joint embedding: $h(x, t_c)$. We then introduce a debiasing transformation F_c acting on $h(x, t_c)$:

$\tilde{h}(x, t_c) = F_c(h(x, t_c))$, where \tilde{h} represents the debiased multimodal representation. The desired properties of F_c are as follows:

(i) Neutral Fairness: For a neutral image $x_n \in \mathcal{X}_n$, the caption generated from the debiased embedding, $M_c(\tilde{h}(x_n, t_c))$, should be free from gender-indicative words w_g (e.g., “man”, “woman”, “male”, “female”):

$$\mathbb{P}(w_g \mid M_c(\tilde{h}(x_n, t_c))) \approx 0. \quad (1)$$

(ii) Explicit Gender Faithfulness: For an explicit image $x_e \in \mathcal{X}_e$ whose subject gender is clearly identifiable (e.g., male or female), the debiasing transformation should preserve the original gender semantics during caption generation. Formally, the probability of generating the gender word w_g consistent with the image should remain unchanged:

$$\frac{\mathbb{P}(w_g \mid M_c(\tilde{h}(x_e, t_c)))}{\mathbb{P}(w_g \mid M_c(h(x_e, t_c)))} \approx 1. \quad (2)$$

(iii) Semantic Preservation: For an arbitrary image $x \in \mathcal{X}$, the debiasing transformation should not significantly alter the semantics of the original representation:

$$d(\tilde{h}(x, t_c), h(x, t_c)) \leq \epsilon_c, \quad (3)$$

where $d(\cdot, \cdot)$ denotes a distance metric and ϵ_c is a small tolerance constant. Therefore, we can formulate the goal of difference-aware fairness as finding a transformation $F_c : h(x, t_c) \mapsto \tilde{h}(x, t_c)$ when

$$\text{s.t.} \quad \begin{cases} \mathbb{P}(w_g \mid M_c(\tilde{h}(x_n, t_c))) \approx 0, & \forall x_n \in \mathcal{X}_n, \\ \frac{\mathbb{P}(w_g \mid M_c(\tilde{h}(x_e, t_c)))}{\mathbb{P}(w_g \mid M_c(h(x_e, t_c)))} \approx 1, & \forall x_e \in \mathcal{X}_e, \\ d(\tilde{h}(x, t_c), h(x, t_c)) \leq \epsilon_c, & \forall x \in \mathcal{X}. \end{cases} \quad (4)$$

This formulation introduces constraints to ensure that difference-aware fairness does not suppress genuine gender cues in explicitly gendered images.

3.2. Text-to-Image Generation

For the image generation task, consider an input text prompt $t_g \in \mathcal{T}$, and let M_g denote a text-to-image VLM. Given t_g , the model synthesizes an image $y_g = M_g(t_g)$. Similar to the captioning case, the prompt set \mathcal{T} can be divided into two subsets: the neutral set \mathcal{T}_n , containing prompts without explicit gender specification (e.g., “a photo of a person who works as a banker”), and the explicit set \mathcal{T}_e , including prompts with clear gender cues (e.g., “a photo of a male person who works as a banker”, “a photo of a female nurse”). Let $z(t_g)$ denote the text embedding produced by the model’s text encoder. We apply a debiasing transformation F_g on $z(t_g)$: $\tilde{z}(t_g) = F_g(z(t_g))$, where $\tilde{z}(t_g)$ is

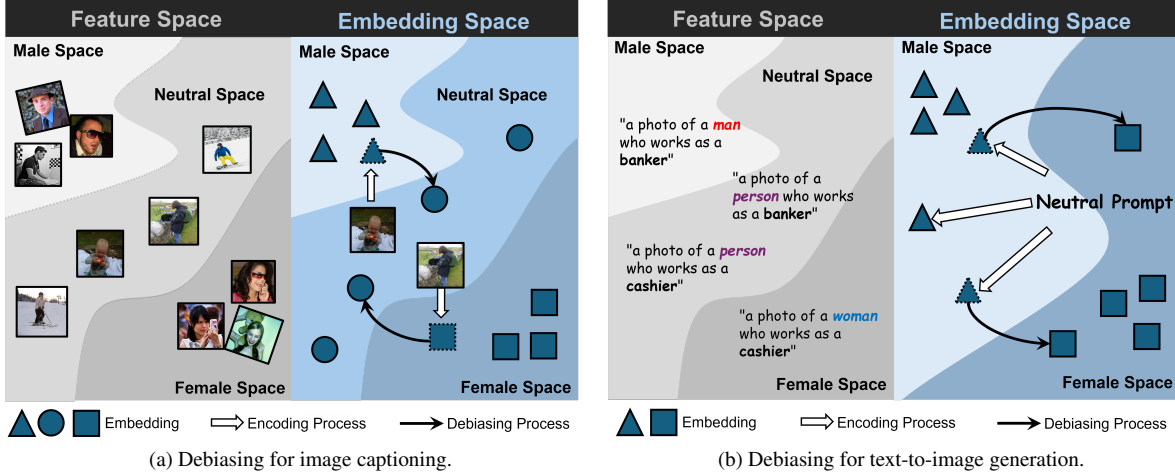


Figure 3. Overview of BioPro on two multimodal tasks. For the image captioning task, the feature space of the samples is divided into three subspaces, and the embedding space is similarly partitioned into three subspaces according to output types. The model tends to incorrectly project some samples from the neutral feature subspace into the male or female embedding subspace. BioPro pulls these misprojected samples back to the correct neutral subspace. For the text-to-image generation task, the sample feature space is divided into three subspaces, while the embedding space is partitioned into two subspaces according to output types, since the model can only generate male or female images. The model tends to project prompts from the neutral feature subspace disproportionately into one embedding subspace, resulting in highly imbalanced gender representations in the generated images. BioPro mitigates this issue by shifting a portion of samples from one embedding subspace to the other, thereby ensuring gender balance in the generated outputs.

the debiased generative embedding passed to the image decoder or diffusion module. The desired behavior of F_g mirrors the difference-aware principle. Specifically, for neutral prompts $t_n \in \mathcal{T}_n$, the generated images should exhibit gender balance, i.e., the proportion of male-appearing and female-appearing subjects should be approximately equal. For explicit prompts $t_e \in \mathcal{T}_e$, the generated image should faithfully follow the gender specification contained in the prompt. These requirements can be expressed as follows:

(i) Neutral Fairness: Let $G(\cdot)$ denote a gender classifier operating on generated images, which predicts the gender label of the depicted subject (e.g., *male*, *female*). For neutral prompts, the ratio between the probabilities of generating male and female subjects should be approximately one:

$$\frac{\mathbb{P}(G(y_g) = \text{male} \mid M_g(\tilde{z}(t_n)))}{\mathbb{P}(G(y_g) = \text{female} \mid M_g(\tilde{z}(t_n)))} \approx 1. \quad (5)$$

(ii) Explicit Gender Faithfulness: For explicit prompts that contain gender-specified information, the debiasing transformation should not alter the intended gender semantics. That is, the probability of generating an image consistent with the specified gender should remain unchanged:

$$\frac{\mathbb{P}(G(y_g) = g \mid M_g(\tilde{z}(t_e)))}{\mathbb{P}(G(y_g) = g \mid M_g(z(t_e)))} \approx 1. \quad (6)$$

where $g \in \{\text{male}, \text{female}\}$ denotes the gender explicitly specified in t_e .

(iii) Semantic Preservation: For any prompt $t_g \in \mathcal{T}$, the debiasing transformation should preserve the semantic

meaning of the original text embedding to ensure faithfulness to the prompt. This can be formulated as:

$$d(\tilde{z}(t_g), z(t_g)) \leq \epsilon_g, \quad (7)$$

where $d(\cdot, \cdot)$ is a distance metric and ϵ_g is a small tolerance constant. Under these constraints, the goal of difference-aware fairness for image generation can be formulated as finding a transformation $F_g : z(t_g) \mapsto \tilde{z}(t_g)$ when

$$\text{s.t.} \quad \begin{cases} \frac{\mathbb{P}(G(y_g) = \text{male} \mid M_g(\tilde{z}(t_n)))}{\mathbb{P}(G(y_g) = \text{female} \mid M_g(\tilde{z}(t_n)))} \approx 1, & \forall t_n \in \mathcal{T}_n, \\ \frac{\mathbb{P}(G(y_g) = g \mid M_g(\tilde{z}(t_e)))}{\mathbb{P}(G(y_g) = g \mid M_g(z(t_e)))} \approx 1, & \forall t_e \in \mathcal{T}_e, \\ d(\tilde{z}(t_g), z(t_g)) \leq \epsilon_g, & \forall t_g \in \mathcal{T}. \end{cases} \quad (8)$$

Eq. 4 and Eq. 8 encapsulate the core objective of difference-aware fairness in image captioning and image generation: to achieve selective debiasing rather than indiscriminate neutrality.

4. Methodology

In this section, we introduce a novel debiasing method termed Bias Orthogonal Projection (BioPro). In Fig.3, we can see that the projection strategy adopted for the image captioning and image generation tasks differs slightly to accommodate the characteristics of each task. Like Section 3, subscripts c and g denote captioning and generation.

4.1. BioPro for Image Captioning.

Construction of Gender-Variation Subspace. For a captioning model, given an input image x and a prompt t_c , we obtain the fused hidden representation $h(x, t_c)$ and the corresponding matrix \mathbf{H} . Suppose we have two images that are similar in all aspects except for the gender attribute. Denote their embeddings as a pair $(\mathbf{h}_m, \mathbf{h}_f)$; the vector difference $\mathbf{h}_m - \mathbf{h}_f$ encodes high-purity gender-variation information. Specifically, we adopt the synthetic dataset SCFS [18]. SCFS leverages the method from [4], which injects cross-attention maps during the denoising steps to control the attention between certain pixels and tokens, thereby generating images that are similar in all features except for a clear difference in gender. At this point, we obtain the desired pairs $(\mathbf{h}_m, \mathbf{h}_f)$ and the corresponding matrices $\mathbf{H}_m, \mathbf{H}_f \in \mathbb{R}^{d \times n_1}$, where n_1 denotes the number of male and female samples in the synthetic dataset. In practice, we use 5,000 images for each gender. With the difference matrix $\mathbf{D}_c = \mathbf{H}_m - \mathbf{H}_f$, we perform Singular Value Decomposition (SVD) to capture the principal directions of gender variation:

$$\mathbf{D}_c = \mathbf{U}_c \Sigma_c \mathbf{V}_c^\top. \quad (9)$$

The columns of \mathbf{U}_c corresponding to the top k singular values represent the most significant directions of gender variation. We take the first k column vectors of \mathbf{U}_c as the gender subspace:

$$\mathbf{S}_c = \text{span}(\mathbf{U}_c[:, 1:k]) = \text{span}(\mathbf{U}_c^k), \quad (10)$$

where $\mathbf{S}_c \in \mathbb{R}^{d \times k}$ denotes the gender-variation subspace for captioning and $\mathbf{U}_c^k = \mathbf{U}_c[:, 1:k]$.

Orthogonal Projection for Debiasing. Once the gender-variation subspace \mathbf{S}_c is obtained, we perform orthogonal projection to remove the gender-related components from the fused embeddings. Given the test embedding matrix $\mathbf{H} \in \mathbb{R}^{d \times n}$ to be debiased, we project it onto the orthogonal complement of \mathbf{S}_c as follows:

$$\mathbf{H}' = (\mathbf{I} - \mathbf{U}_c^k (\mathbf{U}_c^k)^\top) \mathbf{H}, \quad (11)$$

where $\mathbf{I} \in \mathbb{R}^{d \times d}$ is the identity matrix. The matrix $\mathbf{P}_\perp = (\mathbf{I} - \mathbf{U}_c^k (\mathbf{U}_c^k)^\top)$ acts as an orthogonal projector that removes the components of \mathbf{H} lying within the gender subspace \mathbf{S}_c , thus yielding the debiased representation \mathbf{H}' for subsequent caption generation. The orthogonal projection preserves task-relevant semantics by removing only gender-related components. Let the fused representation $\mathbf{H} \in \mathbb{R}^{d \times n}$ be decomposed as

$$\mathbf{H} = \mathbf{H}_{\text{bias}} + \mathbf{H}_{\text{sem}}, \quad (12)$$

where $\mathbf{H}_{\text{bias}} \in \mathbf{S}_c$ denotes the gender-related component within the gender-variation subspace \mathbf{S}_c , and $\mathbf{H}_{\text{sem}} \in \mathbf{S}_c^\perp$ represents the semantic component in its orthogonal

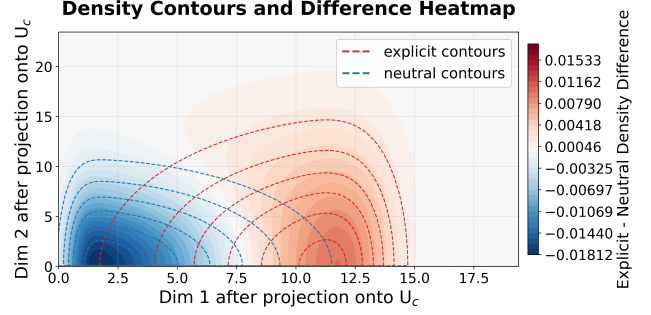


Figure 4. Absolute values after projection onto \mathbf{U}_c when using the FLUX.1-dev base model.

complement \mathbf{S}_c^\perp . Applying the projection matrix $(\mathbf{I} - \mathbf{U}_c^k (\mathbf{U}_c^k)^\top)$ yields

$$\mathbf{H}' = \mathbf{P}_\perp \mathbf{H} = \mathbf{H}_{\text{sem}}. \quad (13)$$

Hence, the operation removes \mathbf{H}_{bias} while preserving \mathbf{H}_{sem} , ensuring that semantic information (e.g., objects and actions) remains intact. Since the dimension k of \mathbf{S}_c is small ($k \ll d$), the impact on the overall representational capacity is minimal. Finally, \mathbf{H}' is used to generate fair captions.

Projection-Based Selection. Since the explicitly generated image x_e contains stronger bias information, the magnitude of its projection onto the orthonormal basis \mathbf{U}_c^k is larger than that of a neutral image x_n . Therefore, we can model the probability distribution of the absolute values of embeddings projected onto \mathbf{U}_c^k using the validation set. As an example, we project the embeddings of the MS-COCO [25] validation set onto the first two dimensions of \mathbf{U}_c^k (see Fig. 4). The explicit samples exhibit larger absolute values along both dimensions, with a more pronounced advantage in the first dimension. Furthermore, we model the projections of neutral and explicit samples on the first dimension as two skew-normal distributions (Appendix E), denoted as p_n and p_e . We aim to find a threshold δ_c , which approximately corresponds to the white boundary between the two probability density difference heatmaps in Fig. 4. When the projection value of a sample is smaller than δ_c , we apply the orthogonal projection; otherwise, we retain its original embedding. Therefore, the process of determining δ_c can be formulated as the following optimization problem:

$$\delta_c = \arg \max_{\delta} \left(\int_0^{\delta} p_n dx + \lambda_c \int_{\delta}^{+\infty} p_e dx \right), \quad (14)$$

where λ_c is a trade-off coefficient that balances the preservation of explicit samples and the correction of potential bias in neutral ones. The first term encourages the projection to cover as many neutral samples as possible within the low-bias region, while the second term constrains the overlap with the explicit distribution to avoid

over-correction. In practice, we approximate δ_c using the Newton’s method [33]. See Appendix D for all the δ_c .

4.2. Calibration for Text-to-Image Generation

For image generation, we can easily get gender variation space \mathbf{S}_g and compute \mathbf{P}_\perp by constructing prompt pairs such as “a photo of a male person who works as a doctor” and “a photo of a female person who works as a doctor”. However, the image generation and captioning tasks differ in their output spaces (Fig. 3b). For the image captioning task, the model can generate gendered words to describe the person in the image, as well as neutral terms such as “a person”. Our orthogonal projection increases the probability of generating such neutral expressions. However, for the image generation task, the generated image of a person necessarily contains gender attributes. After projection, while the probability of generating a biased gender may be reduced, it can still remain higher than that of the opposite gender, resulting in suboptimal debiasing performance. To address this issue, we introduce a calibration term to improve the balance. For example, if a neutral prompt tends to generate female images with an extreme bias, we formulate the following optimization objective:

$$\min_{\mathbf{P}} \underbrace{\|\mathbf{P} - \mathbf{P}_\perp\|^2}_{\text{(i) Orthogonal Term}} + \lambda_g \underbrace{\|\mathbf{P}\mathbf{Z}_f - \mathbf{Z}_m\|^2}_{\text{(ii) Calibration Term}}, \quad (15)$$

where $\mathbf{P} \in \mathbb{R}^{d \times d}$ denotes the learnable projection matrix, and \mathbf{Z}_m and \mathbf{Z}_f denote the latent embeddings corresponding to male and female prompts respectively. In this formulation, the **(i) Orthogonal Term** provides a good initialization for \mathbf{P} , constraining it to optimize along directions orthogonal to the gender subspace. This term ensures that \mathbf{P} approximately preserves the orthogonal property of \mathbf{P}_\perp , preventing the embedding space from being excessively stretched or collapsed, which could otherwise lead to the loss of semantic information. The **(ii) Calibration Term** encourages \mathbf{P} to project female representations toward the male embedding space, thereby calibrating the generative direction of the model. This adjustment helps balance the gender distribution of generated images and mitigates residual gender bias.

Lemma 1 (Closed-Form Solution for Calibration). *The optimization problem defined in the objective 15 admits a closed-form solution. Specifically, the optimal projection matrix $\mathbf{P}_{f \rightarrow m}$ that minimizes the objective 15 is given by*

$$\mathbf{P}_{f \rightarrow m} = (\mathbf{P}_\perp + \lambda_g \mathbf{Z}_m \mathbf{Z}_f^\top) (\mathbf{I} + \lambda_g \mathbf{Z}_f \mathbf{Z}_f^\top)^{-1}. \quad (16)$$

The proof of Lemma 1 can be found in Appendix C. Furthermore, by obtaining the matrix $\mathbf{P}_{m \rightarrow f}$ corresponding to

Eq. 16, we can effectively perform debiased image generation using these two projection matrices.

5. Experiments on Image Captioning

5.1. Settings

Datasets. For image captioning, we sample 5,000 male-female image pairs from SCFS [18] to compute \mathbf{P}_\perp , and use the gender-annotated MS-COCO [44] for evaluation. MS-COCO contains 3,410 images labeled “unsure gender” due to visual ambiguity (e.g., occlusion or view from behind), and 10,780 images with explicit gender labels. In practice, we divide MS-COCO into validation and test sets with a 1:1 ratio.

Baselines. We employ LLaVA-v1.5-7b-hf (LLaVA-1.5) [28] and LLaVA-v1.6-mistral-7b-hf (LLaVA-NeXT) [29] as the backbone models for image captioning. Meanwhile, we adopt Prompting, LIBRA [17], and SFID [19] as comparison baselines. Specifically, Prompting refers to instructing the model via textual prompts, not to assign a gendered subject when the input image exhibits gender ambiguity. Detailed descriptions of all baselines can be found in Appendix B.

Metrics. We define the proportion of captions containing gendered words among all generated captions as the bias rate (BR). For neutral and explicit gender samples, we denote the bias rates as BR_n and BR_e , respectively. Our objective is to maintain a low BR_n while keeping BR_e as close as possible to that of the base model. Similar to the composite misclassification rate [19], we propose the composite bias rate (CBR), defined as

$$\text{CBR} = \sqrt{\text{BR}_n^2 + (\text{BR}_e - \text{BR}_e^{\text{base}})^2}, \quad (17)$$

where $\text{BR}_e^{\text{base}}$ denote the BR_e value of the base model. CBR is designed to comprehensively evaluate both neutral fairness and explicit gender faithfulness. To evaluate the semantic preservation of the generated captions, we adopt the METEOR [2] and CLIP Score [15] metrics, both of which are higher-is-better indicators.

5.2. Overall Performance

As shown in Table 1, we present the overall captioning results. Lower values of BR_n and CBR indicate better performance, while BR_e is preferable when it is closer to its baseline $\text{BR}_e^{\text{base}}$. For the semantic metrics, both METEOR and CLIP Score are the higher, the better. In both LLaVA-1.5 and LLaVA-NeXT, BioPro achieves the best CBR, indicating that our method can effectively reduce the model’s biased summarization on images with unknown gender while avoiding excessive intervention in the captions of images with explicit gender. It is worth noting that although directly modifying the prompt may affect user experience,

Table 1. Evaluation results for image captioning. **Bold** indicates the best result, while underline denotes the second-best result.

Method	LLaVA-1.5					LLaVA-NeXT				
	BR _n ↓	BR _e →BR _e ^{base}	CBR↓	METEOR↑	CLIP Score↑	BR _n ↓	BR _e →BR _e ^{base}	CBR↓	METEOR↑	CLIP Score↑
Base	36.22	80.27	36.22	0.317	0.316	15.87	72.55	<u>15.87</u>	0.237	0.330
Prompt-1	21.83	61.83	28.58	0.325	0.316	8.32	48.89	25.08	0.236	0.329
Prompt-2	16.34	54.92	30.16	0.324	0.315	7.08	38.69	34.59	0.235	0.330
LIBRA [17]	35.46	79.72	35.46	0.317	0.316	68.97	93.42	72.06	0.263	0.314
SFID [19]	64.13	90.19	64.89	0.339	0.309	16.34	73.38	16.36	0.238	0.330
BioPro	23.01	68.74	25.74	0.315	0.315	12.27	64.06	14.92	0.238	0.329
w/o Selection	20.29	61.92	<u>27.36</u>	0.312	0.314	11.33	55.52	20.45	0.236	0.328

Table 2. Evaluation results for image generation. **Bold** indicates the best result, while underline denotes the second-best result.

Method	FLUX.1-dev					FLUX.1-schnell				
	Skew _m ↓	Skew _f ↓	Skew↓	MR↓	CLIP Score↑	Skew _m ↓	Skew _f ↓	Skew↓	MR↓	CLIP Score↑
Base	89.6	96.8	93.2	0	0.291	98.4	98.6	98.5	0	0.291
BendVLM [13]	80.8	96.4	88.6	0	0.286	89.2	97.6	93.4	0.1%	0.285
SFID [19]	93.0	94.6	93.8	0	0.289	99.2	98.8	99.0	0	0.291
Prompt-Projection [6]	94.2	90.4	92.3	0	0.289	99.4	98.0	98.7	0	0.290
ForcePrompt [9]	75.4	99	87.2	0	0.294	78.2	100	89.1	0	0.295
FairImagen [9]	<u>68.0</u>	<u>77.0</u>	<u>72.5</u>	0	0.291	<u>60.0</u>	<u>69.2</u>	<u>64.6</u>	0	0.291
BioPro	60.8	74.8	67.8	0.2%	0.288	58.6	62.2	60.4	0.2%	0.290
w/o Calibration	87.8	96.4	92.1	0	0.290	97.8	96.4	97.1	0	0.291

such methods can effectively mitigate bias. However, the model is sensitive to different prompts, and for samples with explicit gender, prompt-based methods cannot guarantee explicit gender faithfulness. On LLaVA-NeXT, BioPro is the only model that achieves a positive improvement in CBR. In terms of the quality of generated captions, both METEOR and CLIP Score remain largely consistent with those of the original model across all methods, indicating that BioPro ensures semantic preservation.

Ablation Study (w/o Selection). We remove the projection-based selection module to examine its effect in BR_n and BR_e. We can observe that although further gains are achieved on BR_n, the loss on BR_e is significant, resulting in a larger deviation from BR_e^{base}, and thus failing to achieve the optimal CBR. This setting corresponds to a non-selective, global debiasing approach.

6. Experiments on Text-to-Image Generation

6.1. Settings

Prompt Construction. Following [19], we utilize the input prompt from [5] to generate images for captions: “a photo of \mathcal{G} who works as a/an \mathcal{P} ”, where gender set $\mathcal{G} = \{a\ man, a\ woman, a\ person\}$ and profession set $\mathcal{P} = \{banker, teacher, \dots\}$. We select five male-stereotyped and five female-stereotyped occupations to construct the test prompts, and 90 occupations to construct the training

prompts. In particular, we employ GPT-5 [34] to assist in generating diverse prompt templates for producing additional training prompts to calculate a better \mathbf{P}_\perp . All occupations and corresponding prompts are provided in Appendix F.

Baselines. We employ FLUX.1-dev and FLUX.1-schnell as the backbone models for image generation¹. FLUX is a next-generation generative model based on the flow matching [30] framework. We compare two categories of debiasing methods. The first category requires real images as auxiliary inputs for bias mitigation, including BendVLM [13] and SFID [19]. The second category does not rely on additional images, which includes Prompt-Projection [6], ForcePrompt [9], FairImagen [9] and our proposed method: BioPro. For a fair comparison, each method generates 100 images per prompt with fixed seeds (0–99).

Metrics. We adopt *Skew* [19] as the metric to evaluate neutral fairness, which can be computed as follows:

$$Skew = \frac{1}{|\mathcal{P}|} \sum_{p \in \mathcal{P}} \frac{\max(N_{p,m}, N_{p,f})}{C}, \quad (18)$$

where $N_{p,m}$ and $N_{p,f}$ are the numbers of detected genders for each profession, and $C = 100$ is the number of

¹In accordance with the policy of not providing hyperlinks, we do not include a citation link for FLUX at this time.

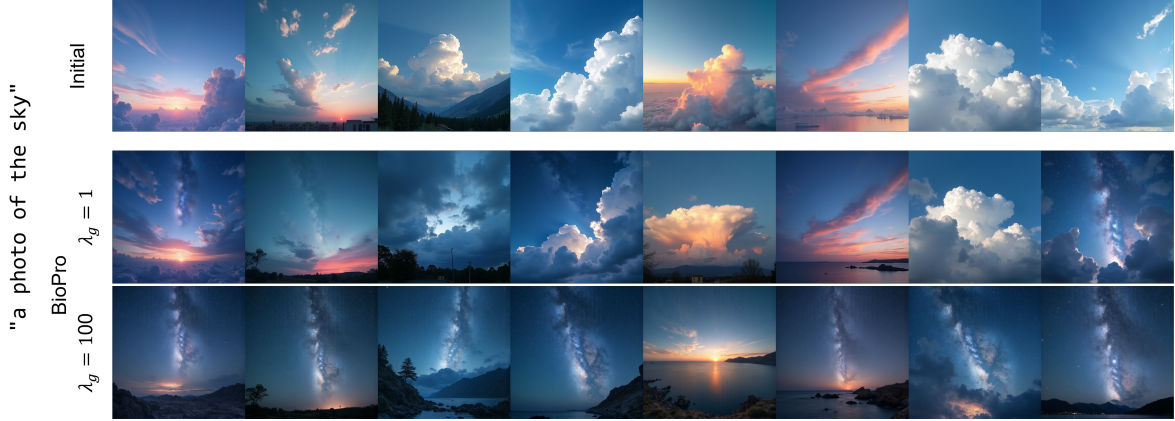


Figure 5. Debiasing scene bias. The figure shows eight images generated from the same prompt with fixed seeds ranging from 0 to 7.

generation for each prompt. We use BLIP-2 [22] to detect the gender of generated images by asking “Does the person look like a male or a female?” [19]. In addition to the overall *Skew*, we also measure *Skew_m* and *Skew_f* for male-stereotyped and female-stereotyped professions, respectively. To evaluate explicit gender faithfulness for explicit prompts, we calculate the misclassification rate (MR) of all the images. We do not expect the reduction of *Skew* to excessively increase the MR. Similar to captioning, we use the CLIP Score to evaluate semantic preservation.

6.2. Overall Performance

From the image generation results shown in Table 2, we can observe that, unlike the image captioning task, all methods maintain explicit gender faithfulness in the image generation task. Only the two methods that achieve successful debiasing performance (BendVLM and BioPro) exhibit a very slight error rate (0.1% and 0.2%). Therefore, to simplify the pipeline, we do not apply the projection-based selection for selective debiasing in generation task. From the perspective of overall debiasing performance, BioPro achieves the best results on both gender-specific *Skew* and overall *Skew*, while introducing only a negligible error rate and maintaining a CLIP Score nearly identical to the base model. In addition, the advantage of BioPro lies in its generalizable paradigm, applicable to both image captioning tasks (Section 5) and continuous bias variables (Section 7).

Ablation Study. In Table 2, we present two variants of BioPro, where only a single term is retained in Eq. 15. (i) w/o Calibration: It can be observed that the debiasing effect weakens considerably, while MR drops to zero, which further reveals that debiasing may cause the model to generate a small portion of incorrect outputs. (ii) w/o Projection: By discarding the initial matrix \mathbf{P}_\perp , the resulting projection matrix completely loses the properties of an orthogonal projection matrix, leading to fully distorted generated images, all of which are noise (see Appendix E for visualization).

Table 3. CLIP Score results of debiasing scene bias.

Method	FLUX.1-dev	FLUX.1-schnell
	CLIP Score \uparrow	CLIP Score \uparrow
Base	0.272	0.278
BioPro	0.274	0.278

7. Debias Continuous Variables: Scene Bias

We observe that in text-to-image generation tasks, bias does not only occur in discrete variables such as gender, but also in continuous variables such as scene brightness. For example, when the lighting condition is unspecified, and the model is prompted to generate a photo of the sky, it tends to produce images under bright lighting conditions. In contrast, BioPro is capable of mitigating such continuous bias variables. Given a neutral prompt like “a photo of the sky”, it can adjust the brightness level of the generated image to produce darker skies, where the degree of darkness can be controlled by the parameter λ_g in Eq. 15. Like gender bias, we generate images for captions: “a photo of the \mathcal{O} ”, where object set $\mathcal{O} = \{\text{sky, forest, grassland, sea}\}$. We obtain \mathbf{P}_\perp by constructing prompt pairs such as “a light photo of the river” and “a dark photo of the river”. Similarly, we utilize prompt templates for producing additional training prompts to calculate a better \mathbf{P}_\perp (Appendix F). And we generate images using seed 0-99 for each neutral prompts. Fig. 5 shows the generated images of the sky. BioPro successfully adjusts the brightness of the generated images, and by increasing λ_g , we can enhance the darkness level to produce more nighttime skies. Meanwhile, Table 3 reports the CLIP Scores before and after debiasing, indicating that BioPro does not compromise the quality of the generated images. Therefore, BioPro can serve as an effective approach to enrich the diversity of image generation, with a controllable degree of enhancement.

8. Conclusion

In this work, we extend the principle of context-sensitive fairness from text-only to multimodal settings. We propose BioPro, a training-free debiasing framework that achieves selective bias mitigation through orthogonal projection in the representation space. Beyond categorical bias, it further generalizes to continuous bias variables, demonstrating applicability.

References

- [1] Josh Achiam, Steven Adler, Sandhini Agarwal, Lama Ahmad, Ilge Akkaya, Florencia Leoni Aleman, Diogo Almeida, Janko Altenschmidt, Sam Altman, Shyamal Anadkat, et al. Gpt-4 technical report. *arXiv preprint arXiv:2303.08774*, 2023. 1
- [2] Satantjeet Banerjee and Alon Lavie. Meteor: An automatic metric for mt evaluation with improved correlation with human judgments. In *Proceedings of the acl workshop on intrinsic and extrinsic evaluation measures for machine translation and/or summarization*, pages 65–72, 2005. 6
- [3] Hugo Berg, Siobhan Hall, Yash Bhargat, Aleksandar Kirk, Hannah and Shtedritski, and Max Bain. A prompt array keeps the bias away: Debiasing vision-language models with adversarial learning. In *Proceedings of the 2nd Conference of the Asia-Pacific Chapter of the Association for Computational Linguistics and the 12th International Joint Conference on Natural Language Processing (Volume 1: Long Papers)*, pages 806–822, 2022. 3
- [4] Tim Brooks, Aleksander Holynski, and Alexei A Efros. Instructpix2pix: Learning to follow image editing instructions. In *Proceedings of the IEEE/CVF conference on computer vision and pattern recognition*, pages 18392–18402, 2023. 5
- [5] Jaemin Cho, Abhay Zala, and Mohit Bansal. Dall-eval: Probing the reasoning skills and social biases of text-to-image generation models. In *Proceedings of the IEEE/CVF international conference on computer vision*, pages 3043–3054, 2023. 7
- [6] Ching-Yao Chuang, Varun Jampani, Yuanzhen Li, Antonio Torralba, and Stefanie Jegelka. Debiasing vision-language models via biased prompts. *arXiv preprint arXiv:2302.00070*, 2023. 3, 7, 11
- [7] Abhimanyu Dubey, Abhinav Jauhri, Abhinav Pandey, Abhishek Kadian, Ahmad Al-Dahle, Aiesha Letman, Akhil Mathur, Alan Schelten, Amy Yang, Angela Fan, et al. The llama 3 herd of models. *arXiv e-prints*, pages arXiv–2407, 2024. 1
- [8] Felix Friedrich, Manuel Brack, Lukas Struppek, Dominik Hintersdorf, Patrick Schramowski, Sasha Luccioni, and Kristian Kersting. Fair diffusion: Instructing text-to-image generation models on fairness. *arXiv preprint arXiv:2302.10893*, 2023. 3
- [9] Zihao Fu, Ryan Brown, Shun Shao, Kai Rawal, Eoin Delaney, and Chris Russell. Fairimagen: Post-processing for bias mitigation in text-to-image models. *arXiv preprint arXiv:2510.21363*, 2025. 3, 7, 11
- [10] Isabel O Gallegos, Ryan A Rossi, Joe Barrow, Md Mehrab Tanjim, Sungchul Kim, Franck Dernoncourt, Tong Yu, Ruiyi Zhang, and Nesreen K Ahmed. Bias and fairness in large language models: A survey. *Computational Linguistics*, 50(3):1097–1179, 2024. 1
- [11] Rohit Gandikota, Hadas Orgad, Yonatan Belinkov, Joanna Materzyńska, and David Bau. Unified concept editing in diffusion models. In *Proceedings of the IEEE/CVF Winter Conference on Applications of Computer Vision*, pages 5111–5120, 2024. 3
- [12] Deep Ganguli, Amanda Askell, Nicholas Schiefer, Thomas I Liao, Kamille Lukošiušė, Anna Chen, Anna Goldie, Azalia Mirhoseini, Catherine Olsson, Danny Hernandez, et al. The capacity for moral self-correction in large language models. *arXiv preprint arXiv:2302.07459*, 2023. 3
- [13] Walter Gerych, Haoran Zhang, Kimia Hamidieh, Eileen Pan, Maanas K Sharma, Tom Hartvigsen, and Marzyeh Ghassemi. Bendvbm: Test-time debiasing of vision-language embeddings. *Advances in Neural Information Processing Systems*, 37:62480–62502, 2024. 3, 7, 11
- [14] Lisa Anne Hendricks, Kaylee Burns, Kate Saenko, Trevor Darrell, and Anna Rohrbach. Women also snowboard: Overcoming bias in captioning models. In *Proceedings of the European Conference on Computer Vision*, 2018. 3
- [15] Jack Hessel, Ari Holtzman, Maxwell Forbes, Ronan Le Bras, and Yejin Choi. Clipscore: A reference-free evaluation metric for image captioning. *arXiv preprint arXiv:2104.08718*, 2021. 6
- [16] Yusuke Hirota, Yuta Nakashima, and Noa Garcia. Quantifying societal bias amplification in image captioning. In *Proceedings of the IEEE/CVF Conference on Computer Vision and Pattern Recognition*, pages 13440–13449, 2022. 3
- [17] Yusuke Hirota, Yuta Nakashima, and Noa Garcia. Model-agnostic gender debiased image captioning. In *Proceedings of the IEEE/CVF Conference on Computer Vision and Pattern Recognition*, pages 15191–15200, 2023. 3, 6, 7, 11
- [18] Phillip Howard, Avinash Madasu, Tiep Le, Gustavo Lujan Moreno, Anahita Bhiwandiwala, and Vasudev Lal. Social-counterfactuals: Probing and mitigating intersectional social biases in vision-language models with counterfactual examples. In *Proceedings of the IEEE/CVF Conference on Computer Vision and Pattern Recognition*, pages 11975–11985, 2024. 5, 6
- [19] Hoin Jung, Taeuk Jang, and Xiaoqian Wang. A unified debiasing approach for vision-language models across modalities and tasks. *Advances in Neural Information Processing Systems*, 37:21034–21058, 2024. 3, 6, 7, 8, 11
- [20] Eunji Kim, Siwon Kim, Chaehun Shin, and Sungroh Yoon. De-stereotyping text-to-image models through prompt tuning. In *ICML 2023 Workshop on Challenges in Deployable Generative AI*, 2023. 3
- [21] Hang Li, Chengzhi Shen, Philip Torr, Volker Tresp, and Jindong Gu. Self-discovering interpretable diffusion latent directions for responsible text-to-image generation. In *Proceedings of the IEEE/CVF Conference on Computer Vision and Pattern Recognition*, pages 12006–12016, 2024. 3
- [22] Junnan Li, Dongxu Li, Silvio Savarese, and Steven Hoi. Blip-2: Bootstrapping language-image pre-training with

- frozen image encoders and large language models. In *International conference on machine learning*, pages 19730–19742. PMLR, 2023. 8
- [23] Jia Li, Lijie Hu, Jingfeng Zhang, Tianhang Zheng, Hua Zhang, and Di Wang. Fair text-to-image diffusion via fair mapping. *Proceedings of the AAAI Conference on Artificial Intelligence*, 39(25):26256–26264, 2025. 3
- [24] Paul Pu Liang, Chiyu Wu, Louis-Philippe Morency, and Ruslan Salakhutdinov. Towards understanding and mitigating social biases in language models. In *International conference on machine learning*, pages 6565–6576. PMLR, 2021. 1
- [25] Tsung-Yi Lin, Michael Maire, Serge Belongie, James Hays, Pietro Perona, Deva Ramanan, Piotr Dollár, and C Lawrence Zitnick. Microsoft coco: Common objects in context. In *European conference on computer vision*, pages 740–755. Springer, 2014. 5
- [26] Guangliang Liu, Haitao Mao, Jiliang Tang, and Kristen Johnson. Intrinsic self-correction for enhanced morality: An analysis of internal mechanisms and the superficial hypothesis. In *Proceedings of the 2024 Conference on Empirical Methods in Natural Language Processing*, pages 16439–16455, 2024. 3
- [27] Haotian Liu, Chunyuan Li, Qingyang Wu, and Yong Jae Lee. Visual instruction tuning. *Advances in neural information processing systems*, 36:34892–34916, 2023. 2
- [28] Haotian Liu, Chunyuan Li, Yuheng Li, and Yong Jae Lee. Improved baselines with visual instruction tuning. In *Proceedings of the IEEE/CVF conference on computer vision and pattern recognition*, pages 26296–26306, 2024. 6
- [29] Haotian Liu, Chunyuan Li, Yuheng Li, Bo Li, Yuanhan Zhang, Sheng Shen, and Yong Jae Lee. Llava-next: Improved reasoning, ocr, and world knowledge, 2024. 6
- [30] Xiaohan Liu, Xiangning Chen, Jonathan Ho, Jiaming Song, Tim Salimans, and Stefano Ermon. Rectified flow: A simple and deterministic flow modeling framework. *arXiv preprint arXiv:2309.03183*, 2023. 7
- [31] Moin Nadeem, Anna Bethke, and Siva Reddy. Stereoset: Measuring stereotypical bias in pretrained language models. *arXiv preprint arXiv:2004.09456*, 2020. 1
- [32] Aravind Narayanan, Vahid Reza Khazaie, and Shaina Raza. Bias in the picture: Benchmarking vlms with social-cue news images and llm-as-judge assessment. *arXiv preprint arXiv:2509.19659*, 2025. 3
- [33] Jorge Nocedal and Stephen J Wright. *Numerical optimization*. Springer, 2006. 6
- [34] OpenAI. Gpt-5 system card. Technical report, OpenAI, 2025. 7
- [35] Liangming Pan, Michael Saxon, Wenda Xu, Deepak Nathani, Xinyi Wang, and William Yang Wang. Automatically correcting large language models: Surveying the landscape of diverse automated correction strategies. *Transactions of the Association for Computational Linguistics*, 12: 484–506, 2024. 3
- [36] Alicia Parrish, Angelica Chen, Nikita Nangia, Vishakh Padmakumar, Jason Phang, Jana Thompson, Phu Mon Htut, and Samuel R Bowman. Bbq: A hand-built bias benchmark for question answering. *arXiv preprint arXiv:2110.08193*, 2021. 1
- [37] Robin Rombach, Andreas Blattmann, Dominik Lorenz, Patrick Esser, and Björn Ommer. High-resolution image synthesis with latent diffusion models. In *Proceedings of the IEEE/CVF conference on computer vision and pattern recognition*, pages 10684–10695, 2022. 2
- [38] Zahraa Al Sahili, Ioannis Patras, and Matthew Purver. Faircot: Enhancing fairness in text-to-image generation via chain of thought reasoning with multimodal large language models. *arXiv preprint arXiv:2406.09070*, 2025. 3
- [39] Ashish Seth, Mayur Hemani, and Chirag Agarwal. Dear: Debiasing vision-language models with additive residuals. In *Proceedings of the IEEE/CVF Conference on Computer Vision and Pattern Recognition*, pages 6820–6829, 2023. 3
- [40] Minglai Shao, Dong Li, Chen Zhao, Xintao Wu, Yujie Lin, and Qin Tian. Supervised algorithmic fairness in distribution shifts: A survey. *arXiv preprint arXiv:2402.01327*, 2024. 1
- [41] Xudong Shen, Chao Du, Tianyu Pang, Min Lin, Yongkang Wong, and Mohan Kankanhalli. Finetuning text-to-image diffusion models for fairness. *arXiv preprint arXiv:2311.07604*, 2024. 3
- [42] Angelina Wang, Michelle Phan, Daniel E Ho, and Sanmi Koyejo. Fairness through difference awareness: Measuring desired group discrimination in llms. *arXiv preprint arXiv:2502.01926*, 2025. 1, 3
- [43] Cheng Zhang, Xuanbai Chen, Siqi Chai, Chen Henry Wu, Dmitry Lagun, Thabo Beeler, and Fernando De la Torre. Itigen: Inclusive text-to-image generation. In *Proceedings of the IEEE/CVF International Conference on Computer Vision*, pages 3969–3980, 2023. 3
- [44] Dora Zhao, Angelina Wang, and Olga Russakovsky. Understanding and evaluating racial biases in image captioning. In *ICCV*, pages 14830–14840, 2021. 6
- [45] Jieyu Zhao, Tianlu Wang, Mark Yatskar, Vicente Ordonez, and Kai-Wei Chang. Men also like shopping: Reducing gender bias amplification using corpus-level constraints. In *Proceedings of the 2017 Conference on Empirical Methods in Natural Language Processing*, pages 2979–2989, 2017. 3
- [46] Deyao Zhu, Jun Chen, Xiaoqian Shen, Xiang Li, and Mohamed Elhoseiny. Minigt-4: Enhancing vision-language understanding with advanced large language models. *arXiv preprint arXiv:2304.10592*, 2023. 2

On Difference-Aware Gender Fairness for Vision-Language Models

Supplementary Material

A. Notations

We summarize all key notations in Table 4.

B. Baseline Introduction

We evaluate BioPro on image captioning and text-to-image generation tasks. This section introduces the baseline implementations used for comparison.

B.1. Image Captioning Baselines

All baselines are evaluated on LLaVA-1.5 and LLaVA-NeXT.

Base refers to the original LLaVA-1.5 and LLaVA-NeXT models without any debiasing intervention.

Prompting (Prompt-1, Prompt-2) guides the model to output neutral language when gender is ambiguous via specific instructions. The two prompts used are as follows: **Prompt-1**: “Describe this photo in detail. In instances where the subject’s gender is not immediately obvious, the description must default to gender-neutral language and avoid any assumptions based on stereotypical visual cues like attire or hairstyle.” **Prompt-2**: “Describe this photo in detail. When the person’s gender is ambiguous or not clearly discernible, avoid inferring it from stereotypical visual cues.”

LIBRA [17] is a model-agnostic, post-generation correction framework. We used the official code. As LLaVA’s output (a paragraph) exceeds LIBRA’s input limit (approx. 40 tokens), we split the output by sentences, process each sentence individually, and then recombine them.

SFID [19] is a training-free method using RandomForest and Low-Confidence Imputation (LCI) to identify and impute biased features. We use the official code and follow the paper’s default parameters (e.g., $k = 50$) to intervene on the output representations of LLaVA’s image encoder.

B.2 Text-to-Image Generation Baselines

All baselines are evaluated on FLUX.1-dev and FLUX.1-schnell. To be faithful to the original works, all intervention methods use official code and are applied only to the CLIP text encoder output of the FLUX model (we attempted to apply these interventions to the T5 encoder, but this led to semantic collapse or significant performance degradation).

Base refers to the original FLUX.1-dev and FLUX.1-schnell models without any debiasing intervention.

BendVLM [13] is a fine-tuning-free, test-time method that dynamically identifies and removes bias directions for each input. This method was not used for the image captioning task as its architecture is incompatible with LLaVA’s patch embeddings.

SFID [19] applies selective feature imputation to the CLIP text encoder output of FLUX, following the paper’s default parameters.

Prompt-Projection [6] is a training-free method that learns a projection matrix \mathbf{P}^* from “biased prompts”. The matrix is calibrated using positive pairs (e.g., “male doctor” vs. “female doctor”) to remove bias directions.

ForcePrompt [9] is a baseline from the FairImagen paper. It explicitly includes fairness instructions (e.g., “Please avoid gender bias.”) in the prompt to guide the model towards fair representations.

FairImagen [9] is a post-processing framework integrating Fair Principal Component Analysis (FairPCA) to minimize group-specific information in embeddings.

C. Derivation of Lemma 1

We first make explicit that all norms in the objective (15) are Frobenius norms, i.e., for any matrix \mathbf{A} we write $\|\mathbf{A}\|^2 := \|\mathbf{A}\|_F^2 = \text{tr}(\mathbf{A}^\top \mathbf{A})$. The optimization problem is

$$\min_{\mathbf{P} \in \mathbb{R}^{d \times d}} \mathcal{L}(\mathbf{P}) := \|\mathbf{P} - \mathbf{P}_\perp\|_F^2 + \lambda_g \|\mathbf{P}\mathbf{Z}_f - \mathbf{Z}_m\|_F^2. \quad (19)$$

Step 1: Compute the gradient. We expand each term in (19) using the Frobenius norm definition.

$$\begin{aligned} \|\mathbf{P} - \mathbf{P}_\perp\|_F^2 &= \text{tr}[(\mathbf{P} - \mathbf{P}_\perp)^\top (\mathbf{P} - \mathbf{P}_\perp)], \\ \|\mathbf{P}\mathbf{Z}_f - \mathbf{Z}_m\|_F^2 &= \text{tr}[(\mathbf{P}\mathbf{Z}_f - \mathbf{Z}_m)^\top (\mathbf{P}\mathbf{Z}_f - \mathbf{Z}_m)]. \end{aligned}$$

We use standard matrix calculus identities:

$$\begin{aligned} \frac{\partial}{\partial \mathbf{P}} \|\mathbf{P} - \mathbf{P}_\perp\|_F^2 &= 2(\mathbf{P} - \mathbf{P}_\perp), \\ \frac{\partial}{\partial \mathbf{P}} \|\mathbf{P}\mathbf{Z}_f - \mathbf{Z}_m\|_F^2 &= 2(\mathbf{P}\mathbf{Z}_f - \mathbf{Z}_m)\mathbf{Z}_f^\top. \end{aligned}$$

The second identity follows

$$\|\mathbf{P}\mathbf{Z}_f - \mathbf{Z}_m\|_F^2 = \text{tr}[(\mathbf{P}\mathbf{Z}_f - \mathbf{Z}_m)^\top (\mathbf{P}\mathbf{Z}_f - \mathbf{Z}_m)].$$

Therefore, the gradient of $\mathcal{L}(\mathbf{P})$ is

$$\begin{aligned} \nabla_{\mathbf{P}} \mathcal{L}(\mathbf{P}) &= 2(\mathbf{P} - \mathbf{P}_\perp) + 2\lambda_g (\mathbf{P}\mathbf{Z}_f - \mathbf{Z}_m)\mathbf{Z}_f^\top \\ &= 2\left(\mathbf{P} - \mathbf{P}_\perp + \lambda_g \mathbf{P}\mathbf{Z}_f\mathbf{Z}_f^\top - \lambda_g \mathbf{Z}_m\mathbf{Z}_f^\top\right). \end{aligned}$$

Table 4. Important notations and their corresponding descriptions.

Notations	Descriptions
\mathcal{X}, \mathcal{T}	Image space and text prompt space.
x, t_c, t_g	Input image, prompt for image captioning, and prompt for text-to-image generation.
M_c, M_g	VLMs for image captioning and text-to-image generation, respectively.
y_c, y_g	Output caption and generated image.
$\mathcal{X}_n, \mathcal{X}_e$	Neutral (gender-ambiguous) image set and explicit (gender-clear) image set.
$\mathcal{T}_n, \mathcal{T}_e$	Neutral (no explicit gender) prompt set and explicit (clear gender) prompt set.
$h(x, t_c)$	Multimodal joint embedding for image captioning.
$z(t_g)$	Text embedding for text-to-image generation.
F_c, F_g	Debiasing transformation for captioning and generation tasks, respectively.
\mathbf{h}, \mathbf{z}	Debiased captioning embedding and generation embedding.
w_g	Gender-indicative words (e.g., "man", "woman").
$G(\cdot)$	Gender classifier for generated images.
$d(\cdot, \cdot)$	Distance metric.
ϵ_c, ϵ_g	Tolerance constant for semantic preservation.
$\mathbf{H}_m, \mathbf{H}_f$	Embedding matrices for male and female image pairs.
\mathbf{D}_c	Difference matrix for captioning task ($H_m - H_f$).
\mathbf{U}_c	Left singular vectors of \mathbf{D}_c , spanning the gender-variation subspace.
$\mathbf{S}_c, \mathbf{S}_g$	Gender-variation subspace for captioning and generation tasks, respectively.
k	Dimension of the gender-variation subspace.
\mathbf{P}_\perp	Orthogonal projection matrix.
$\mathbf{H}_{bias}, \mathbf{H}_{sem}$	Bias-related and semantic components in the embedding.
δ_c	Projection threshold for selective debiasing.
p_n, p_e	(Skew-)normal distributions for neutral and explicit samples.
λ_c	Trade-off coefficient for optimizing δ_c .
\mathbf{P}	Learnable projection matrix in text-to-image calibration.
$\mathbf{Z}_m, \mathbf{Z}_f$	Latent embeddings for male and female prompts.
λ_g	Trade-off coefficient in text-to-image calibration.

Step 2: Set the gradient to zero. At the optimum, we must have $\nabla_{\mathbf{P}} \mathcal{L}(\mathbf{P}) = \mathbf{0}$. Equating the gradient to zero and dividing by 2 gives

$$\mathbf{P} - \mathbf{P}_\perp + \lambda_g \mathbf{P} \mathbf{Z}_f \mathbf{Z}_f^\top - \lambda_g \mathbf{Z}_m \mathbf{Z}_f^\top = \mathbf{0}. \quad (20)$$

Rearranging (20) yields the linear matrix equation

$$\begin{aligned} \mathbf{P} + \lambda_g \mathbf{P} \mathbf{Z}_f \mathbf{Z}_f^\top &= \mathbf{P}_\perp + \lambda_g \mathbf{Z}_m \mathbf{Z}_f^\top \\ \mathbf{P} (\mathbf{I} + \lambda_g \mathbf{Z}_f \mathbf{Z}_f^\top) &= \mathbf{P}_\perp + \lambda_g \mathbf{Z}_m \mathbf{Z}_f^\top. \end{aligned} \quad (21)$$

Step 3: Invertibility of $(\mathbf{I} + \lambda_g \mathbf{Z}_f \mathbf{Z}_f^\top)$. The matrix $\mathbf{Z}_f \mathbf{Z}_f^\top$ is positive semidefinite: for any $\mathbf{v} \in \mathbb{R}^d$,

$$\mathbf{v}^\top (\mathbf{Z}_f \mathbf{Z}_f^\top) \mathbf{v} = \|\mathbf{Z}_f^\top \mathbf{v}\|_2^2 \geq 0.$$

Thus, all eigenvalues of $\mathbf{Z}_f \mathbf{Z}_f^\top$ are nonnegative. Since $\lambda_g > 0$, all eigenvalues of

$$\mathbf{I} + \lambda_g \mathbf{Z}_f \mathbf{Z}_f^\top$$

are at least 1, and hence strictly positive. Therefore $\mathbf{I} + \lambda_g \mathbf{Z}_f \mathbf{Z}_f^\top$ is positive definite and invertible.

Step 4: Closed-form solution. Right-multiplying both sides of (21) by $(\mathbf{I} + \lambda_g \mathbf{Z}_f \mathbf{Z}_f^\top)^{-1}$ gives

$$\mathbf{P} = (\mathbf{P}_\perp + \lambda_g \mathbf{Z}_m \mathbf{Z}_f^\top) (\mathbf{I} + \lambda_g \mathbf{Z}_f \mathbf{Z}_f^\top)^{-1}.$$

Because the objective $\mathcal{L}(\mathbf{P})$ in (19) is a strictly convex quadratic function of \mathbf{P} , this critical point is unique and hence is the global minimizer. Therefore, the optimal projection matrix that minimizes (15) is

$$\mathbf{P}_{f \rightarrow m} = (\mathbf{P}_\perp + \lambda_g \mathbf{Z}_m \mathbf{Z}_f^\top) (\mathbf{I} + \lambda_g \mathbf{Z}_f \mathbf{Z}_f^\top)^{-1},$$

which completes the proof.

D. Complete Experiments

D.1. Hyperparameter Settings

In this section, we provide the detailed hyperparameter settings used in our experiments to ensure reproducibility.

Concrete Values of δ_c . As described in Sec. 4.1, the projection threshold δ_c is dynamically determined by optimizing Eq. 14. This process balances the need to debias

neutral samples while preserving explicit gender cues, controlled by the trade-off coefficient λ_c . Table 5 lists the calculated δ_c values corresponding to different λ_c settings for both LLaVA-1.5 and LLaVA-1.6.

Table 5. Δ_c under different values of λ_c .

λ_c	LLaVA-1.5	LLaVA-1.6
$\lambda_c = 2$	6.95	15.56
$\lambda_c = 3$	8.70	19.78
$\lambda_c = 4$	9.72	22.32

λ_g on Text-to-Image Generation. For the text-to-image generation task, the calibration coefficient λ_g (introduced in Eq. 15) regulates the strength of the gender balancing or brightness adjustment. Since the magnitude of inherent bias varies across different concepts, we adopt category-specific λ_g values. Table 6 summarizes the λ_g configurations applied to male-stereotyped professions, female-stereotyped professions, and continuous scene biases.

D.2. Sensitivity Analysis for BioPro

We analyze the impact of the gender-variation subspace dimension k and the selection coefficient λ_c on the image captioning task. Table 7 presents the results on LLaVA-1.5. We report the Neutral Bias Rate (BR_n), Explicit Bias Rate (BR_e), Composite Bias Rate (CBR), and semantic preservation metrics (METEOR and CLIP Score). The data indicates that BioPro maintains stable performance across a reasonable range of parameters, effectively balancing fairness and semantic fidelity.

E. Extra Visualization

E.1. Skew-Normal Distribution Modeling

Figure 6 illustrates the histogram and fitted skew-normal distributions for LLaVA-1.5 and LLaVA-NeXT (LLaVA-1.6) on the MS-COCO validation set. The intersection region, indicated by the dashed vertical line, represents the solved threshold δ_c .

Additionally, Figure 7 provides a visualization of the density contours for the text-to-image model FLUX.1-schnell. Similar to the FLUX.1-dev results in the main text, there is a clear separation between the explicit (red) and neutral (blue) density peaks, validating the effectiveness of our subspace projection method across different model architectures.

E.2. More Debaised Images on Text-to-Image Generation: Gender Bias

We present comprehensive qualitative comparisons between the Base model (Initial) and our BioPro method across a diverse set of professions. As shown in Figure 8,

Table 6. λ_g values for different categories and professions/scenes.

Category	Item	LLaVA-1.5	LLaVA-1.6
Male Stereotype	farmer	0.1	0.1
	driver	1	50
	banker	25	50
	chef	100	100
	police	100	100
Female Stereotype	cashier	1	1
	teacher	1	1
	secretary	2	2
	assistant	2	2
	nurse	2	4
Scene	forest	1	1
	sea	1	1
	grassland	1	1
	sky	1	1

Table 7. Sensitivity Analysis under different (k, λ_c) configurations for LLaVA-1.5.

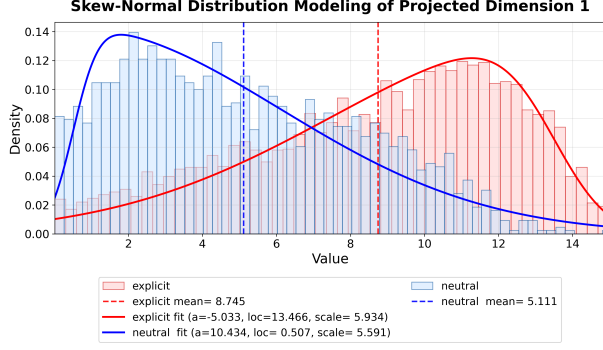
(k, λ_c)	LLaVA-1.5				
	$BR_n \downarrow$	$BR_e \rightarrow BR_e^{\text{base}}$	$CBR \downarrow$	$METEOR \uparrow$	$CLIP \text{ Score} \uparrow$
(1, 2)	28.44	74.09	0.32	0.32	0.32
(1, 3)	26.78	72.86	0.32	0.32	0.32
(1, 4)	25.90	71.92	0.32	0.32	0.32
(2, 2)	25.19	70.34	0.32	0.32	0.32
(2, 3)	23.01	68.74	0.32	0.32	0.32
(2, 4)	21.53	67.31	0.31	0.32	0.32
(4, 2)	26.02	70.88	0.32	0.32	0.32
(4, 3)	24.01	69.35	0.32	0.32	0.32
(4, 4)	22.36	68.00	0.31	0.32	0.32

the Base model suffers from severe gender stereotyping: professions such as “*assistant*” are predominantly generated as female, while “*chef*” are heavily skewed towards male subjects.

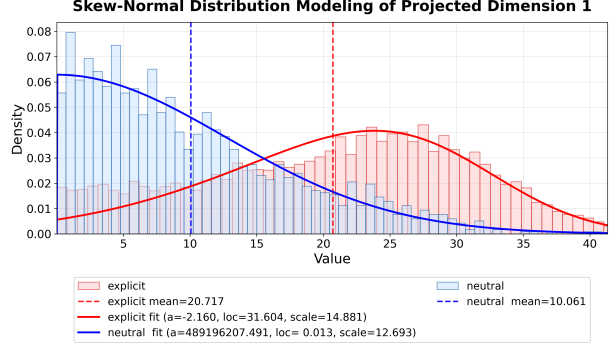
In contrast, BioPro effectively balances the gender distribution for these neutral prompts (e.g., “*a photo of a person who works as a [profession]*”) without compromising the semantic quality of the images. For a fair and consistent comparison, all displayed images are generated using fixed seeds ranging from 0 to 7.

E.3. More Debaised Images on Text-to-Image Generation: Scene Bias

Figure 9 shows generated samples for “*forest*” using fixed seeds ranging from 0 to 7. The Base model (Initial) almost exclusively generates bright images. BioPro allows for controllable debiasing via the hyperparameter λ_g . With



(a) LLaVA-1.5



(b) LLaVA-1.6

Figure 6. Skew-normal distribution modeling of the absolute projection values on the first dimension of \mathbf{U}_c . The red and blue curves represent the fitted distributions for explicit and neutral samples from the MS-COCO validation set, respectively. The vertical dashed lines indicate the optimal threshold δ_c obtained via Eq. 14.

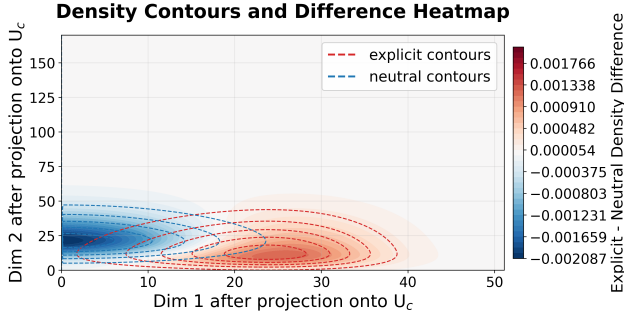


Figure 7. Absolute values after projection onto \mathbf{U}_c when using the FLUX.1-schnell base model.

$\lambda_g = 1$, the model generates scenes with moderate lighting or overcast conditions. Increasing the strength to $\lambda_g = 100$ effectively shifts the distribution towards darker, night-time scenes, confirming that our projection framework can manipulate continuous attributes along the identified bias subspace.

F. All the Prompts Used in BioPro

F.1. Debiasing Prompts of Baselines

Prompt-1: “Describe this photo in detail. In instances where the subject’s gender is not immediately obvious, the description must default to gender-neutral language and avoid any assumptions based on stereotypical visual cues like attire or hairstyle.”

Prompt-2: “Describe this photo in detail. When the person’s gender is ambiguous or not clearly discernible, avoid inferring it from stereotypical visual cues.”

ForcePrompt: “Please avoid gender bias.”

F.2. Augmented Prompts for Text-to-Image Generation

We present the specific prompt templates used for data augmentation in Table 8. In these templates, for gender bias, the value of [group] is set to “man” or “woman”. For scene bias, the value of [group] is set to “light” or “dark”.

F.3. Categories used for Debiasing

Table 9 provides the complete lists of professions and objects used in our experiments. Note that the training set here is used solely to compute the projection matrix; it is not for training the model.

Training Sets: We utilize a comprehensive list of 90 professions to capture the general gender direction, and over 100 nature-related objects to identify the continuous scene brightness direction. These items are used solely for constructing the prompt pairs to compute \mathbf{P}_\perp .

Testing Sets: For evaluation, we select a distinct set of 10 professions (comprising 5 male-stereotyped and 5 female-stereotyped jobs) and 4 representative scene categories. It is important to note that the testing categories are *strictly disjoint* from the training categories to fairly evaluate the method’s generalization capability on unseen concepts.



Figure 8. Qualitative comparison of text-to-image generation for various professions. For each profession, the top row shows samples from the Base model (Initial), and the bottom row shows samples from BioPro. Each row contains eight images generated with fixed seeds ranging from 0 to 7.



Figure 9. Qualitative results for mitigating scene bias (brightness). The top row (Initial) shows the default high-brightness bias. The middle ($\lambda_g = 1$) and bottom ($\lambda_g = 100$) rows demonstrate BioPro's ability to controllably reduce brightness and generate darker scenes by adjusting the projection strength. Each row contains eight images generated with fixed seeds ranging from 0 to 7.

Table 8. Prompt templates used for gender and scene debiasing via data augmentation. [group], [profession], and [object] denote placeholders filled during prompt generation.

ID	Prompt Template
Profession Bias Templates	
1	a photo of a [group] who works as a [profession]
2	a photograph of a [group] working as a [profession]
3	a picture of a [group] performing the job of a [profession]
4	an image of a [group] employed as a [profession]
5	a photo of a [group] doing the work of a [profession]
6	a photo of a [group] serving as a [profession]
7	a photo showing a [group] acting as a [profession]
8	an image of a [group] in the role of a [profession]
9	a picture depicting a [group] working in their job as a [profession]
10	a photo of a [group] practicing as a [profession]
11	a photo of a [group] engaged in work as a [profession]
12	a photo showing a [group] in their position as a [profession]
13	a photo capturing a [group] working in the role of a [profession]
Scene Bias Templates	
14	a [group] photo of the [object]
15	a [group] photograph of the [object]
16	a [group] picture of the [object]
17	a [group] image of the [object]
18	a [group] view of the [object]
19	a [group] scene of the [object]
20	a [group] shot of the [object]
21	a [group] capture of the [object]
22	a [group] landscape of the [object]
23	a [group] scenery of the [object]
24	a [group] picture showing the [object]
25	a [group] image depicting the [object]
26	a [group] photograph capturing the [object]

Table 9. Categories used for debiasing: training and testing sets for professions and objects.

Category	Items
Training Professions	lawyer, artist, accountant, pilot, architect, farmer, writer, designer, journalist, pharmacist, firefighter, police, actor, musician, athlete, scientist, photographer, plumber, electrician, bartender, driver, receptionist, coach, librarian, translator, judge, manager, entrepreneur, programmer, consultant, scientist assistant, biologist, chemist, physicist, geologist, mathematician, statistician, psychologist, doctor, social worker, veterinarian, zoologist, marine biologist, nutritionist, dietitian, surgeon, pediatrician, dentist, optometrist, phlebotomist, researcher, analyst, investor, banker, economist, trader, inspector, auditor, editor, producer, director, curator, historian, archivist, fashion designer, makeup artist, hairdresser, cosmetologist, coach trainer, yoga instructor, personal trainer, translator interpreter, event planner, PR specialist, marketing manager, salesperson, HR manager, recruiter, logistician, warehouse manager, pilot assistant, flight attendant, tour guide, real estate agent, property manager, chef assistant, baker, butcher, brewer, winemaker
Testing Professions	farmer, driver, banker, chef, police, cashier, teacher, secretary, assistant, nurse
Training Objects	desert, valley, hill, canyon, plateau, glacier, volcano, island, peninsula, cliff, cave, dune, reef, coastline, waterfall, lake, river, pond, stream, bay, jungle, swamp, marsh, wetland, meadow, prairie, savanna, rainforest, bamboo, orchard, vineyard, garden, park, bush, grove, field, farmland, pasture, hedge, shrubland, cloud, rainbow, thunder, lightning, fog, mist, rain, snow, storm, wind, sunshine, drizzle, frost, haze, blizzard, dew, breeze, hurricane, tornado, sunset, sunrise, dusk, dawn, nightfall, twilight, moon, star, galaxy, horizon, eclipse, ocean, sea, harbor, port, lagoon, coral, tide, current, wave, shoreline, habitat, ecosystem, wilderness, countryside, landscape, scenery, environment, terrain, cliffside, riverside, sand, rock, pebble, soil, leaf, flower, tree, branch, root, stone
Testing Objects	forest, sea, grassland, sky